Journal of Cerebral Blood Flow & Metabolism (2015) 35, 1380–1385

www.jcbfm.com

ORIGINAL ARTICLE

Reduced uptake of ^{18}F-FDG and ^{15}O-H_2O in Alzheimer's disease-related regions after glucose loading

Kenji Ishibashi, Keiichi Kawasaki, Kiichi Ishiwata and Kenji Ishii

Increased plasma glucose levels are known to reduce fluorine-18-labeled fluorodeoxyglucose (^{18}F-FDG) uptake in Alzheimer's disease (AD)-related regions, resulting in the appearance of an AD-like pattern. However, the relationships of its appearance with cerebral blood flow and insulin levels are uncertain. We performed ^{18}F-FDG and oxygen-15-labeled water (^{15}O-H_2O) positron emission tomography in the fasting and glucose-loading conditions on nine young healthy volunteers with no cognitive impairments. Measurement of plasma glucose and insulin levels confirmed that all subjects were free of insulin resistance, and that glucose loading significantly increased plasma glucose and insulin levels. Fluorine-18-labeled fluorodeoxyglucose and ^{15}O-H_2O images were compared between the two conditions, focusing on AD-related regions: precuneus/posterior cingulate (PP), lateral parietal cortex (LPC), and frontal cortex (FC). Volume-of-interest analyses showed significantly lower uptake of both ^{18}F-FDG and ^{15}O-H_2O in PP, LPC, and FC after glucose loading ($P < 0.05$). Whole-brain voxel-wise analyses also revealed the PP, LPC, and FC areas where uptake of both ^{18}F-FDG and ^{15}O-H_2O decreased ($P < 0.05$, familywise error rate-corrected). We concluded that increased plasma glucose and insulin levels can cause the appearance of the AD-like pattern in both ^{18}F-FDG and ^{15}O-H_2O images, and this phenomenon can occur even in subjects without insulin resistance.

Journal of Cerebral Blood Flow & Metabolism (2015) **35,** 1380–1385; doi:10.1038/jcbfm.2015.127; published online 10 June 2015

Keywords: ^{18}F-FDG; ^{15}O-H_2O; Alzheimer's disease; glucose; insulin

INTRODUCTION

The positron emission tomography (PET) radioligand, fluorine-18-labeled fluorodeoxyglucose (^{18}F-FDG), is used to estimate regional cerebral metabolic rates of glucose utilization ($rCMR_{glc}$), which reflect the regional brain activities that are associated with physiologic or pathophysiologic conditions.[1] Because the absolute measurements of $rCMR_{glc}$ require arterial blood sampling, which is an invasive procedure and which leads to high intersubject and intrasubject variability in the $rCMR_{glc}$ values,[2] the measurement of ^{18}F-FDG uptake without arterial blood sampling, which has smaller intersubject and intrasubject variability, has been widely used in neuroimaging studies as well as in clinical practice for the differential diagnosis of patients with dementia.[3,4] However, cerebral ^{18}F-FDG uptake is affected by plasma glucose levels because of the competition with glucose for the transporters and hexokinase.[5] Thus, instead of providing a quantitative assessment of $rCMR_{glc}$, this method quantitatively assesses the changes in the distribution pattern of ^{18}F-FDG, which is possibly associated with physical or pathologic conditions.

Patients with Alzheimer's disease (AD) show prominent reduction in ^{18}F-FDG uptake in the precuneus/posterior cingulate (PP), parietotemporal, and frontal regions.[6,7] This characteristic distribution pattern of ^{18}F-FDG is described as an AD pattern, and is useful for the diagnosis of AD. Interestingly, recent studies showed that increased plasma glucose levels, even in cognitively normal subjects, can alter the cerebral distribution pattern of ^{18}F-FDG and reduce ^{18}F-FDG uptake in AD-related regions,[8,9] resulting in the appearance of the AD-like pattern. In addition, a more recent study showed that the AD-like pattern observed during a hyperglycemic state can be reversible and independent of amyloid-β deposition or apolipoprotein E ε4 genotype.[10] Another study showed that the AD-like pattern can appear even at fasting plasma glucose levels of 100 to 110 mg/dL.[11]

Oxygen-15-labeled water (^{15}O-H_2O) is another radioligand used in PET to estimate regional cerebral blood flow (rCBF), which is related to regional brain activity. Patients with AD also show the AD pattern in CBF images as observed in ^{18}F-FDG images.[12] However, it is uncertain whether the AD-like pattern during a hyperglycemic state also appears in CBF images. Additionally, measurements of plasma insulin levels are lacking in the previous studies of ^{18}F-FDG. Because insulin affects brain function[13] and may modify the AD-related pathology,[14] its measurement may provide essential information for understanding the AD-like pattern. The goal of this study was to address these issues. We measured the plasma glucose and insulin levels before and after glucose loading and examined the changes in the distribution pattern of ^{18}F-FDG and ^{15}O-H_2O, testing the hypothesis that glucose loading reduces the uptake of both radioligands in AD-related regions leading to the appearance of the AD-like pattern. Additionally, we discuss the link between glucose, insulin, insulin resistance, and the AD-like pattern.

Research Team for Neuroimaging, Tokyo Metropolitan Institute of Gerontology, Tokyo, Japan. Correspondence: Dr K Ishibashi, Research Team for Neuroimaging, Tokyo Metropolitan Institute of Gerontology, 35-2 Sakae-cho, Itabashi-ku, Tokyo 173-0015, Japan.
E-mail: ishibashi@pet.tmig.or.jp
This work was supported in part by Nakayama Foundation for Human Science (to KIshibashi).
Received 7 March 2015; revised 14 May 2015; accepted 18 May 2015; published online 10 June 2015

MATERIALS AND METHODS

Research Participants

The study was conducted in accordance with Helsinki Protocol, and approved by the Ethics Committee of the Tokyo Metropolitan Institute of Gerontology. After a detailed explanation of the study, each participant provided written informed consent. The sample was composed of nine volunteers (6 men and 3 women; mean age = 21.7 years, s.d. = 1.5, range = 20 to 25). None of the subjects had a history of diabetes, and all were defined as healthy based on a medical interview with a neurologist, physical, and neurologic examination results, and findings from magnetic resonance imaging (MRI).

Study Protocol

The study protocol is summarized in Figure 1. Each subject visited our institute twice to undergo ^{18}F-FDG and ^{15}O-H_2O PET scans in two different conditions: the fasting condition (first visit) and the glucose-loading condition (second visit). The time interval between the two visits was 2 or 3 weeks. On the day of the first visit, participants fasted for more than 5 hours before the injection of the first dose of ^{15}O-H_2O, which was followed by the second dose of ^{15}O-H_2O, and then ^{18}F-FDG. On the day of the second visit, 2 to 3 hours after lunch, each subject was administered 50 g glucose orally (TRELAN-G50, 150 mL; AY Pharma, Tokyo, Japan) 30 minutes before the injection of the first dose of ^{15}O-H_2O, which was followed by the second dose of ^{15}O-H_2O, and then ^{18}F-FDG. The time intervals between the first and second injections of ^{15}O-H_2O, and between the second injection of ^{15}O-H_2O and the injection of ^{18}F-FDG, were 10 minutes and 15 minutes, respectively.

The plasma glucose level was measured twice at the time of the ^{18}F-FDG injection with a medical device (FDC100G; Fujifilm, Tokyo, Japan), and the two values were averaged. The measurement system was based on the glucose oxidase-peroxidase method. The plasma insulin level was measured once at the time of the injection with the enzyme immunoassay method (SRL, Inc., Tokyo, Japan). An index of insulin resistance, Homeostasis model assessment of Insulin Resistance (HOMA-IR), was calculated by the following formula: HOMA-IR = (fasting glucose (mg/dL) × fasting insulin (μU/mL))/405.

Positron Emission Tomography Scanning

The radioligands, ^{18}F-FDG and ^{15}O-H_2O, were synthesized with a PET tracer automatic production system (Sumitomo Heavy Industries, Ltd., Tokyo, Japan). The radiochemical purity of ^{18}F-FDG and ^{15}O-H_2O was more than 95% and 100%, respectively. The PET scanning was performed using a SET-2400 W scanner (Shimadzu, Kyoto, Japan) in three-dimensional mode at the Tokyo Metropolitan Institute of Gerontology. Images with 63 slices were obtained with a 2.054 × 2.054 × 3.125 mm^3 voxel size and a 128 × 128 matrix size. The transmission data were acquired with a rotating ^{68}Ga/^{68}Ge rod source for measured attenuation correction. The injected dose was 150 MBq for both ^{18}F-FDG and ^{15}O-H_2O. Static emission data for ^{18}F-FDG were acquired for 45 to 51 minutes after intravenous bolus injection. Meanwhile, to measure the uptake of ^{15}O-H_2O with less noise, two ^{15}O-H_2O scans were conducted with a 10-minute interscanning interval to allow for decay (Figure 1). Each ^{15}O-H_2O scan was started upon the appearance of radioactivity in the brain after an intravenous bolus injection of ^{15}O-H_2O. Static ^{15}O-H_2O emission data were then acquired for 60 seconds in one frame.[15,16] Data were reconstructed after correction for decay, attenuation, and scatter.

Positron Emission Tomography Image Processing and Volumes-of-Interest

All participants underwent MRI scanning in three-dimensional mode (3DSPGR; repetition time 9.2 ms; echo time 2.0 ms; matrix size 256 × 256 × 124; voxel size 0.94 × 0.94 × 1.3 mm^3). The images were processed using the FMRIB Software Library version 5.0.4 (FSL; Oxford University, Oxford, UK), and were used for the subsequent PET image processing. Each subject had one ^{18}F-FDG and two ^{15}O-H_2O images for each condition (Figure 1). The two ^{15}O-H_2O images were realigned and averaged to reduce noise. The ^{18}F-FDG and ^{15}O-H_2O images were then coregistered to the corresponding structural MRI (FSL FLIRT), and transformed into the Montreal Neurological Institute (MNI) space from native space using MRI-guided spatial normalization (FSL FNIRT). The warped ^{18}F-FDG and ^{15}O-H_2O images in MNI space were smoothed with a 4-mm sigma Gaussian kernel. Cortical and subcortical regions were masked using the MNI structural atlas (included in FSL), and proportionally scaled to a global mean value (mean value = 100) that was computed on the masked voxels. The normalized image representing the uptake of ^{18}F-FDG or ^{15}O-H_2O was finally completed, and used for the subsequent volume-of-interest (VOI)-based and voxel-wise analyses.

Volumes-of-interest were carefully defined on PP, lateral parietal cortex (LPC), and frontal cortex (FC) as representative AD-related regions in MNI space (Figure 2). To create these VOIs, we used ^{18}F-FDG PET data from 15 patients with AD and 31 age-matched healthy controls that belong to a database at the Tokyo Metropolitan Institute of Gerontology. The study using the data has been published elsewhere.[11] Briefly, the first step was the detection of clusters representing glucose hypometabolic regions in AD by using voxel-wise analyses between the 15 AD patients and 31 controls. Next, each cluster was extracted at the appropriate level of statistical threshold depending on its location to include a large enough

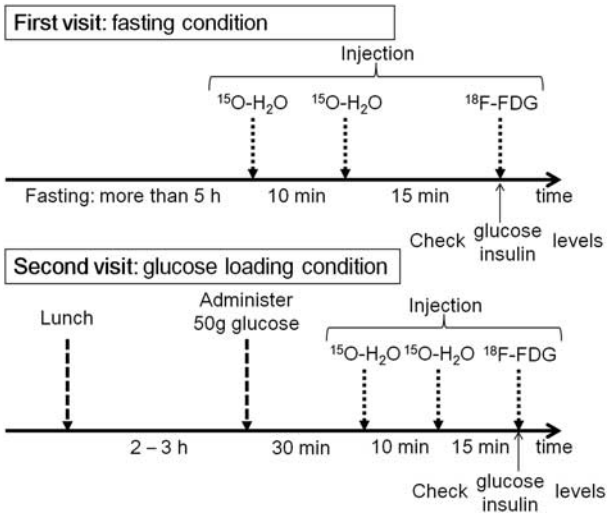

Figure 1. Diagram of the study protocol. Each subject visited our institute twice to undergo fluorine-18-labeled fluorodeoxyglucose (^{18}F-FDG) and oxygen-15-labeled water (^{15}O-H_2O) positron emission tomography (PET) scans in two different conditions: fasting and glucose loading.

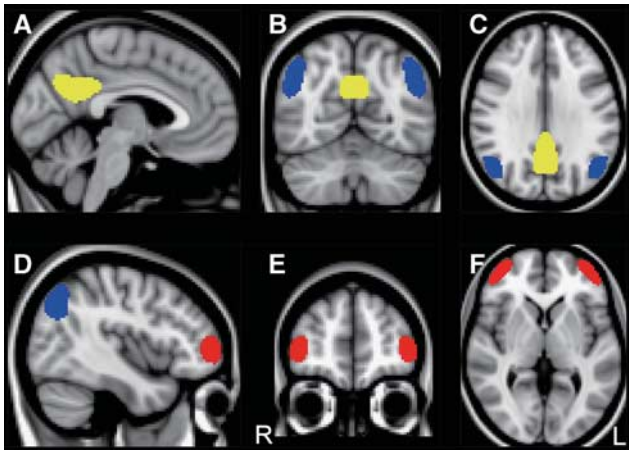

Figure 2. Volumes-of-interest (VOIs) in MNI space. VOIs placed on the precuneus/posterior cingulate (yellow), lateral parietal cortex (blue), and frontal cortex (red) are displayed on a MNI standard brain in sagittal (**A** and **D**), coronal (**B** and **E**), and axial (**C** and **F**) sections. The MNI coordinates (x, y, z mm) for upper (**A**–**C**) and lower (**D**–**F**) panels were (−4, −62, 30) and (42, 50, 2), respectively. L, left; MNI, Montreal Neurological Institute; R, right.

number of voxels. Then, its shape was modified to be symmetrical. Volumes-of-interest for PP, LPC, and FC were finally completed in MNI space (Figure 2). The VOI volumes were 1,263, 1,640, and 988 voxels for PP, LPC, and FC, respectively.

Data Analysis and Statistical Analysis

The VOI-based analyses were performed to assess the effect of glucose loading on the uptake of ^{18}F-FDG and ^{15}O-H_2O in AD-related regions. The VOIs for PP, LPC, and FC were moved on the normalized ^{18}F-FDG and ^{15}O-H_2O images in MNI space, and the uptake values on the VOIs were extracted. We tested the differences in the uptake of ^{18}F-FDG or ^{15}O-H_2O in each AD-related region between the fasting and glucose-loading conditions using a one-tailed paired *t*-test. The null hypothesis was that the uptake of ^{18}F-FDG or ^{15}O-H_2O in each AD-related region did not decrease from the fasting to glucose-loading conditions. Statistical significance was set at $P < 0.05$.

Exploratory whole-brain voxel-wise analyses were then performed to corroborate the results of VOI-based analyses and to find every region where glucose loading altered the distribution pattern of both ^{18}F-FDG and ^{15}O-H_2O and decreased the uptake of both radioligands, using Statistical Parametric Mapping, version 12 (SPM12; Wellcome Trust Center for Neuroscience, London, UK) implemented in MATLAB, version R2014a (The MathWorks, Natick, MA, USA). We specified a full factorial design, consisting of a 2×2 design with repeated measures (2 radioligands $\times$ 2 conditions). Statistical *t* map of '^{18}F-FDG (fasting): 1, ^{18}F-FDG (glucose loading): –1, ^{15}O-H_2O (fasting): 1 and ^{15}O-H_2O (glucose loading): -1' contrast was calculated using a height threshold of $P < 0.05$, familywise error rate (FWE)-corrected, excluding clusters smaller than 50 voxels. The SPM *t* map was transformed to the *P* map.

RESULTS

The plasma glucose and insulin levels in the fasting and glucose-loading conditions, as well as the HOMA-IR values for the nine subjects are summarized in Table 1. These data confirmed that all subjects were free of insulin resistance and diabetes. After glucose loading, there was a significant increase in the levels of plasma glucose ($P = 0.002$, $T = 3.92$) and insulin ($P < 0.001$, $T = 8.06$) using a one-tailed paired *t*-test.

The results from VOI-based analyses are shown in Table 2. After glucose loading, there was significantly lower uptake of ^{18}F-FDG in PP ($P < 0.001$, $T = 4.75$), LPC ($P < 0.001$, $T = 5.28$), and FC ($P < 0.001$, $T = 4.80$), and that of ^{15}O-H_2O in PP ($P = 0.004$, $T = 3.49$), LPC ($P = 0.032$, $T = 2.15$), and FC ($P = 0.025$, $T = 2.32$). The decreasing uptakes of ^{18}F-FDG were 5.7%, 4.5%, and 3.7%, and those of ^{15}O-H_2O were 2.1%, 1.4%, and 1.7% in PP, LPC, and FC, respectively. A representative case is displayed in Figure 3 (subject 3 in Table 2), where both ^{18}F-FDG and ^{15}O-H_2O uptake decreased especially in the PP after glucose loading.

Exploratory whole-brain SPM analyses revealed three clusters at $P < 0.05$ ($T > 5.05$), FWE-corrected, located in the PP, LPC, and FC areas (Figure 4). The MNI coordinates of each peak-level voxel in the three clusters were included in the PP, LPC, and FC VOIs that we specified as AD-related regions.

Table 1. Plasma glucose and insulin levels in nine young volunteers

Subject	*Age (years)*	*Sex*	*Fasting condition*			*Glucose-loading condition*	
			Glucose (mg/dL)	*Insulin* (μU/mL)	*HOMA-IR*	*Glucose (mg/dL)*	*Insulin (μU/mL)*
1	25	F	79.5	1.05	0.21	104.5	91.6
2	22	F	88.0	6.51	1.41	100.0	75.4
3	22	M	78.0	2.22	0.43	104.5	125.0
4	22	M	82.0	3.36	0.68	92.5	53.4
5	21	M	87.0	7.69	1.65	109.5	61.8
6	21	F	84.5	5.54	1.16	106.5	127.0
7	20	M	87.5	4.35	0.94	123.0	48.5
8	22	M	80.5	5.14	1.02	103.0	72.7
9	20	M	82.5	2.49	0.51	167.5	94.9
Mean	21.7		83.3	4.26	0.89	112.3	83.4
s.d.	1.5		3.7	2.17	0.48	22.2	28.7

HOMA-IR, Homeostasis model assessment of Insulin Resistance; s.d., standard deviation.

Table 2. Uptake values of ^{18}F-FDG and ^{15}O-H_2O in the fasting and glucose-loading conditions

Region	*Fasting condition*		*Glucose-loading condition*		P-*value*	T-*value*
	Mean	*s.d.*	*Mean*	*s.d.*		
^{18}F-FDG						
PP	151.1	5.8	142.4	6.1	< 0.001	4.75
LPC	118.7	6.0	113.4	4.5	< 0.001	5.28
FC	102.7	4.8	98.9	5.0	< 0.001	4.80
^{15}O-H_2O						
PP	137.3	4.4	134.4	4.4	0.004	3.49
LPC	104.7	4.6	103.2	4.2	0.032	2.15
FC	91.6	2.5	90.0	3.1	0.025	2.32

^{18}F-FDG, fluorine-18-labeled fluorodeoxyglucose; ^{15}O-H_2O, oxygen-15-labeled water; FC, frontal cortex; LPC, lateral parietal cortex; PP, precuneus/posterior cingulate. *P*-and *T*-values from a one-tailed paired *t*-test between the fasting and glucose-loading conditions.

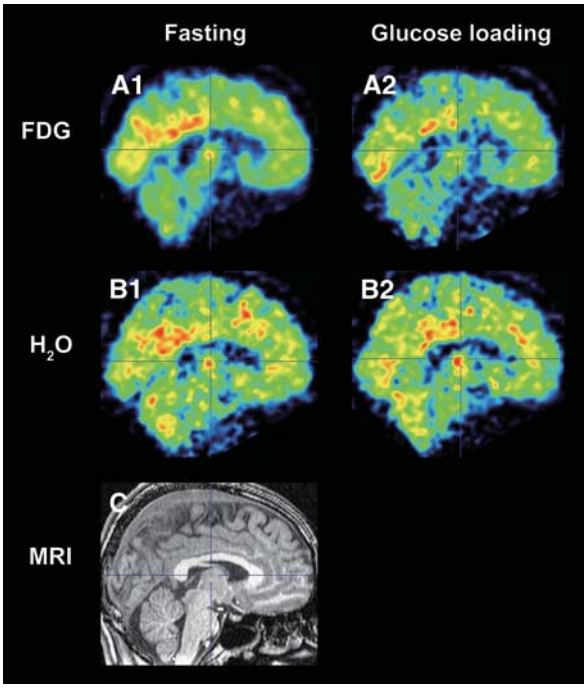

Figure 3. A representative case of fluorine-18-labeled fluorodeoxyglucose (^{18}F-FDG) and oxygen-15-labeled water (^{15}O-H_2O) images. The ^{18}F-FDG (**A1** and **A2**) and ^{15}O-H_2O (**B1** and **B2**) images coregistered to the corresponding magnetic resonance imaging (MRI) (**C**) are displayed in sagittal sections. This case was from subject 3 in Table 2.

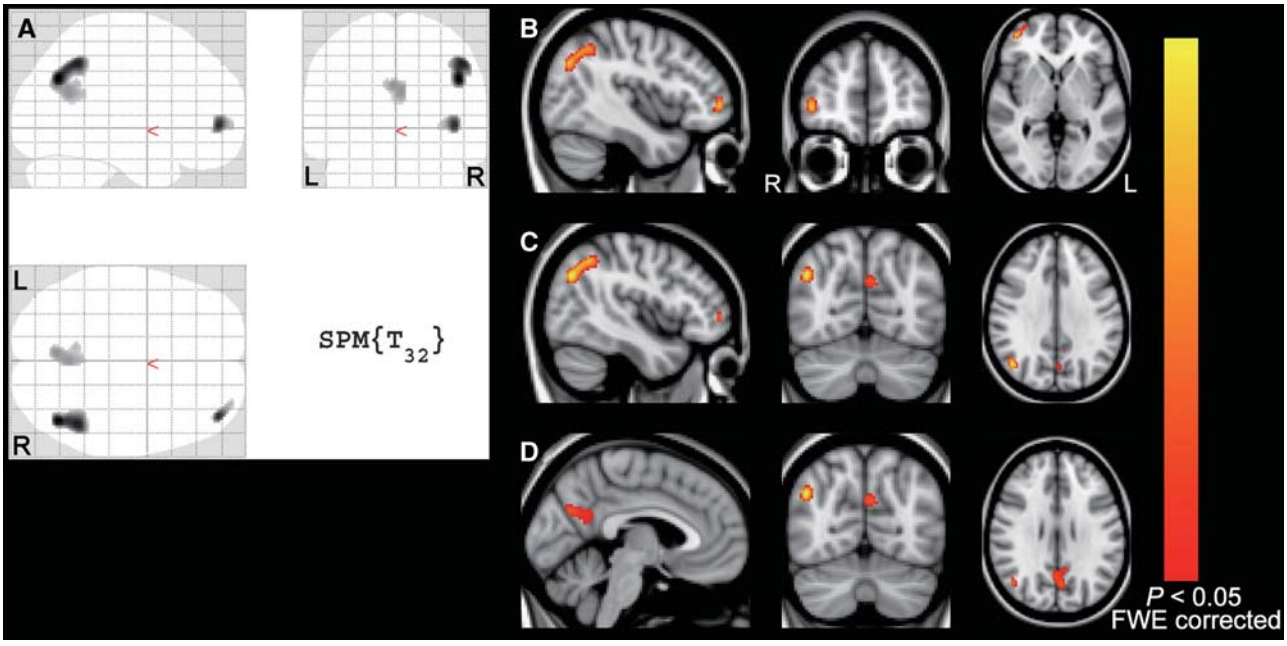

Figure 4. Results of whole-brain voxel-wise analyses. Three significant clusters at $P < 0.05$, FWE-corrected (T value > 5.05) are displayed on SPM glass brain (**A**) and on MNI standard brain with MNI coordinates of each of the three peak-level voxels (**B**–**D**). MNI coordinates (x, y, z mm) for (**B**), (**C**), and (**D**) were (42, 50, 0), (44, −68, 32), and (−4, −68, 28), respectively. The yellow–red scale represents magnitude of P values. FWE, familywise error rate; L, left; R, right.

DISCUSSION

Increased plasma glucose levels can alter the cerebral distribution pattern of ^{18}F-FDG from normal to AD-like in cognitively normal subjects.[8,9,11] In an ^{18}F-FDG PET study of nine healthy older subjects, glucose loading yielded the appearance of the AD-like pattern.[8] The AD-like pattern after glucose loading can be reversible, and independent of amyloid-β deposition and the apolipoprotein E ε4 genotype.[10] In a cross-sectional study of 124 cognitively normal older subjects, higher fasting plasma glucose levels were significantly correlated with the magnitude of reduced uptake of ^{18}F-FDG in AD-related regions.[9] The AD-like pattern in the fasting condition can appear even in an individual with mildly higher levels of fasting plasma glucose, from 100 to 110 mg/dL.[11] The VOI-based and voxel-wise analyses in this study provided additional findings that glucose loading alters the distribution pattern of ^{18}F-FDG as well as ^{15}O-H_2O and reduces the uptake of both radioligands in AD-related regions leading to the appearance of the AD-like pattern, and that the ^{18}F-FDG images may have relatively higher sensitivity for the detection of the AD-like pattern than ^{15}O-H_2O images.

The present study showed that the decreasing uptakes of ^{18}F-FDG and ^{15}O-H_2O were 3.7% to 5.7% and 1.4% to 2.1%, respectively, in the AD-related regions. According to the recent diagnostic guidelines for AD,[17] the clinical stages of AD are classified into the preclinical, mild cognitive impairment, and dementia stages. The ^{18}F-FDG uptake, which is a marker for synaptic dysfunction, may start to decrease in the preclinical AD stage, and its uptake in AD-related regions continues to decrease along with disease progression.[17] Actually, the magnitude of the reductions in ^{18}F-FDG uptake and CBF in AD-related regions is greater in the dementia stage than in the mild cognitive impairment stage.[7,18] When the ^{18}F-FDG data were collected from 15 patients with AD whose Mini-Mental State Examination scores were around 20 and who belonged to a database at the Tokyo Metropolitan Institute of Gerontology, ^{18}F-FDG uptake in the PP area was decreased by roughly 25% compared with controls.[11] The magnitude of the reductions can depend on how the ^{18}F-FDG uptake values are normalized. However, based on previous reports,[7,11,17] the amounts of the decreased uptake of ^{18}F-FDG and ^{15}O-H_2O that were observed in this study were definitely small compared with those in patients with typical AD but may be comparable to some patients in the mild cognitive impairment or early dementia stage. Therefore, we suggest that it is essential to pay attention to at least plasma glucose levels when diagnosing AD with ^{18}F-FDG or CBF images to avoid image misinterpretation.

Increased plasma glucose levels are known to cause changes in glucose transport and enzyme hexokinase activity to preserve glucose consumption leading to changes in the kinetic constants (K_1, k_2, and k_3).[19] Since ^{18}F-FDG uses the same transporters and the same enzyme hexokinase, the kinetic constants of ^{18}F-FDG change in the same way. Additionally, ^{18}F-FDG competes with glucose for the transporters and hexokinase.[5] Thus, hyperglycemia reduces the cerebral uptake of ^{18}F-FDG,[20–23] although global CMR_{glc} in a whole brain may be unchanged.[19,24–26] The effects of hyperglycemia on the cerebral uptake of ^{15}O-H_2O have not been investigated to our knowledge, although global CBF in a whole brain have been reported to be unchanged[26] or decreased.[27–29] However, experimental studies with rats showed that induction of hyperglycemia affected both $rCMR_{glc}$ and rCBF, and that the magnitude of changes in $rCMR_{glc}$ and rCBF during a hyperglycemic state was different between brain regions in cortical and subcortical gray matter and white matter,[19,27] indicating that induction of hyperglycemia can alter the distribution pattern of both $rCMR_{glc}$ and rCBF in a whole brain. The mechanisms underlying the reductions in rCBF during hyperglycemia may be a result of increased cerebrovascular resistance from plasma hyperosmolality, increased blood viscosity, and decreased $rCMR_{glc}$.[27] In this study, we assessed the changes in the distribution pattern of ^{18}F-FDG and ^{15}O-H_2O, using relative values from a global normalization method. Our observations may suggest that the PP, LPC, and FC areas are vulnerable to hyperglycemia in human brain.

Increased insulin levels are usually observed with increased plasma glucose levels,[30,31] and their increase in the fasting condition is associated with greater insulin resistance.[32] Since insulin affects glucose utilization in the central nervous system,[33,34] it has an important role in modulating regional brain activity. Baker *et al*[35]

recently reported that in 23 cognitively normal patients with prediabetes or early type-2 diabetes, greater insulin resistance was associated with reduced uptake of ^{18}F-FDG in AD-related regions.[35] In their study, mean levels of fasting blood glucose and insulin in the patient group were 107.1 mg/dL (mildly increased) and 17.1 μU/mL (moderately increased), respectively, leading to an increase in the index of insulin resistance, HOMA-IR. Meanwhile, the young volunteers in this study were free of insulin resistance in the fasting condition; however, reductions in ^{18}F-FDG and ^{15}O-H_2O uptake were observed in AD-related regions with increased levels of plasma glucose and insulin after glucose loading. Our current observations are fundamentally consistent with those of Baker *et al*, but additionally provided initial evidence that the appearance of the AD-like pattern can occur with increased levels of plasma glucose and insulin, independent of whether an individual has insulin resistance or not. To understand the relationships of the AD-like pattern with the two factors of glucose and insulin, further studies that investigate which factor is more likely to explain the appearance of the AD-like pattern are needed.

The PP, LPC, and FC areas overlap with the functional anatomy of the default mode network (DMN).[36] The DMN is characterized by high activity when the mind is not engaged in specific behavioral tasks and low activity during focused attention on the external environment, and has an important role in regulating complex cognition and behavior.[37–39] Its functional connectivity is impaired in patients with AD and asymptomatic older individuals with amyloid-β accumulation,[40] and its impairment is associated with current and future cognitive decline.[41] Interestingly, the functional connectivity in the DMN also decreases in cognitively normal patients with diabetes.[42] This shared vulnerability of the DMN between diabetes and AD may be a vital component of the link between increased plasma glucose and insulin levels and the appearance of the AD-like pattern in ^{18}F-FDG and ^{15}O-H_2O images.

There are some limitations in this study. First, the sample size was relatively small. Since the ^{15}O-H_2O images were created by only 1 minute of scanning, they included a certain amount of noise that might reduce statistical power in VOI-based analyses from ^{15}O-H_2O images compared with those from ^{18}F-FDG images. Second, no randomization was used in the setup of the study. Therefore, systemic bias effects may have been present. Another limitation was that we used relative values to quantitatively assess the changes in the distribution patterns of ^{18}F-FDG and ^{15}O-H_2O uptake because the method has smaller intersubject and intrasubject variability than the absolute values of $rCMR_{glc}$, this substantially increases the statistical power.[2] However, it is essential to quantitatively assess $rCMR_{glc}$ to understand the phenomena observed in the study. Our results need to be replicated in future studies with a larger sample size, randomization, arterial blood sampling, and kinetic analysis for quantitative assessment of $rCMR_{glc}$ and rCBF.

CONCLUSION

This study showed that glucose loading altered the distribution pattern of both ^{18}F-FDG and ^{15}O-H_2O and reduced the uptake of both radioligands in AD-related brain regions, suggesting that increased plasma and insulin levels induce the appearance of an AD-like pattern in both ^{18}F-FDG and ^{15}O-H_2O images. This study also provides initial evidence that the phenomenon can occur even in subjects without insulin resistance.

AUTHOR CONTRIBUTIONS

KK and K Ishii designed research and performed research; K Ishibashi and K Ishii analyzed data; K Ishibashi, KK, K Ishiwata, and K Ishii wrote the paper.

DISCLOSURE/CONFLICT OF INTEREST

The authors declare no conflict of interest.

ACKNOWLEDGMENTS

The authors thank Ms. Hiroko Tsukinari and Mr. Kunpei Hayashi for their technical assistance.

REFERENCES

1 Phelps ME, Huang SC, Hoffman EJ, Selin C, Sokoloff L, Kuhl DE. Tomographic measurement of local cerebral glucose metabolic rate in humans with (F-18)2-fluoro-2-deoxy-D-glucose: validation of method. *Ann Neurol* 1979; **6**: 371–388.
2 Wang GJ, Volkow ND, Wolf AP, Brodie JD, Hitzemann RJ. Intersubject variability of brain glucose metabolic measurements in young normal males. *J Nucl Med* 1994; **35**: 1457–1466.
3 Yakushev I, Hammers A, Fellgiebel A, Schmidtmann I, Scheurich A, Buchholz HG *et al.* SPM-based count normalization provides excellent discrimination of mild Alzheimer's disease and amnestic mild cognitive impairment from healthy aging. *NeuroImage* 2009; **44**: 43–50.
4 Suhonen-Polvi H, Ruotsalainen U, Kinnala A, Bergman J, Haaparanta M, Teras M *et al.* FDG-PET in early infancy: simplified quantification methods to measure cerebral glucose utilization. *J Nucl Med* 1995; **36**: 1249–1254.
5 Wienhard K. Measurement of glucose consumption using [(18)F]fluorodeoxyglucose. *Methods* 2002; **27**: 218–225.
6 Friedland RP, Budinger TF, Ganz E, Yano Y, Mathis CA, Koss B *et al.* Regional cerebral metabolic alterations in dementia of the Alzheimer type: positron emission tomography with [18 F]fluorodeoxyglucose. *J Comput Assist Tomogr* 1983; **7**: 590–598.
7 Langbaum JB, Chen K, Lee W, Reschke C, Bandy D, Fleisher AS *et al.* Categorical and correlational analyses of baseline fluorodeoxyglucose positron emission tomography images from the Alzheimer's Disease Neuroimaging Initiative (ADNI). *NeuroImage* 2009; **45**: 1107–1116.
8 Kawasaki K, Ishii K, Saito Y, Oda K, Kimura Y, Ishiwata K. Influence of mild hyperglycemia on cerebral FDG distribution patterns calculated by statistical parametric mapping. *Ann Nucl Med* 2008; **22**: 191–200.
9 Burns CM, Chen K, Kaszniak AW, Lee W, Alexander GE, Bandy D *et al.* Higher serum glucose levels are associated with cerebral hypometabolism in Alzheimer regions. *Neurology* 2013; **80**: 1557–1564.
10 Ishibashi K, Miura Y, Oda K, Ishiwata K, Ishii K. Alzheimer's disease-like pattern of (18)F-FDG uptake during a hyperglycemic state and negative (11)C-PiB binding in a patient with mild cognitive impairment. *J Alzheimer's Dis* 2014; **42**: 385–389.
11 Ishibashi K, Onishi A, Fujiwara Y, Ishiwata K, Ishii K. Relationship between Alzheimer disease-like pattern of 18 F-FDG and fasting plasma glucose levels in cognitively normal volunteers. *J Nucl Med* 2015; **56**: 229–233.
12 Matsuda H. Cerebral blood flow and metabolic abnormalities in Alzheimer's disease. *Ann Nucl Med* 2001; **15**: 85–92.
13 Gray SM, Meijer RI, Barrett EJ. Insulin regulates brain function, but how does it get there? *Diabetes* 2014; **63**: 3992–3997.
14 Matsuzaki T, Sasaki K, Tanizaki Y, Hata J, Fujimi K, Matsui Y *et al.* Insulin resistance is associated with the pathology of Alzheimer disease: the Hisayama study. *Neurology* 2010; **75**: 764–770.
15 Raichle ME, Martin WR, Herscovitch P, Mintun MA, Markham J. Brain blood flow measured with intravenous H2(15)O. II. Implementation and validation. *J Nucl Med* 1983; **24**: 790–798.
16 Poline JB, Vandenberghe R, Holmes AP, Friston KJ, Frackowiak RS. Reproducibility of PET activation studies: lessons from a multi-center European experiment. EU concerted action on functional imaging. *NeuroImage* 1996; **4**: 34–54.
17 Sperling RA, Aisen PS, Beckett LA, Bennett DA, Craft S, Fagan AM *et al.* Toward defining the preclinical stages of Alzheimer's disease: recommendations from the National Institute on Aging-Alzheimer's Association workgroups on diagnostic guidelines for Alzheimer's disease. *Alzheimers Dement* 2011; **7**: 280–292.
18 Binnewijzend MA, Kuijer JP, Benedictus MR, van der Flier WM, Wink AM, Wattjes MP *et al.* Cerebral blood flow measured with 3D pseudocontinuous arterial spin-labeling MR imaging in Alzheimer disease and mild cognitive impairment: a marker for disease severity. *Radiology* 2013; **267**: 221–230.
19 Orzi F, Lucignani G, Dow-Edwards D, Namba H, Nehlig A, Patlak CS *et al.* Local cerebral glucose utilization in controlled graded levels of hyperglycemia in the conscious rat. *J Cereb Blood Flow Metab* 1988; **8**: 346–356.
20 Wahl RL, Henry CA, Ethier SP. Serum glucose: effects on tumor and normal tissue accumulation of 2-[F-18]-fluoro-2-deoxy-D-glucose in rodents with mammary carcinoma. *Radiology* 1992; **183**: 643–647.
21 Hara T, Higashi T, Nakamoto Y, Suga T, Saga T, Ishimori T *et al.* Significance of chronic marked hyperglycemia on FDG-PET: is it really problematic for clinical oncologic imaging? *Ann Nucl Med* 2009; **23**: 657–669.

22 Yamada K, Endo S, Fukuda H, Abe Y, Yoshioka S, Itoh M *et al.* Experimental studies on myocardial glucose metabolism of rats with 18 F-2-fluoro-2-deoxy-D-glucose. *Eur J Nucl Med* 1985; **10**: 341–345.
23 Marian T, Balkay L, Fekete I, Lengyel Z, Veress G, Esik O *et al.* Hypoglycemia activates compensatory mechanism of glucose metabolism of brain. *Acta Biol Hung* 2001; **52**: 35–45.
24 Brondsted HE, Gjedde A. Glucose phosphorylation rate in rat parietal cortex during normoglycemia, hypoglycemia, acute hyperglycemia, and in diabetes-prone rats. *Acta Neurol Scand* 1990; **81**: 233–236.
25 Duckrow RB, Bryan RM, Jr. Regional cerebral glucose utilization during hyperglycemia. *J Neurochem* 1987; **48**: 989–993.
26 Hasselbalch SG, Knudsen GM, Capaldo B, Postiglione A, Paulson OB. Blood-brain barrier transport and brain metabolism of glucose during acute hyperglycemia in humans. *J Clin Endocrinol Metab* 2001; **86**: 1986–1990.
27 Duckrow RB, Beard DC, Brennan RW. Regional cerebral blood flow decreases during chronic and acute hyperglycemia. *Stroke* 1987; **18**: 52–58.
28 Harik SI, LaManna JC. Vascular perfusion and blood-brain glucose transport in acute and chronic hyperglycemia. *J Neurochem* 1988; **51**: 1924–1929.
29 Knudsen GM, Tedeschi E, Jakobsen J. The influence of haematocrit and blood glucose on cerebral blood flow in normal and in diabetic rats. *Neuroreport* 1992; **3**: 987–989.
30 Cambien F, Warnet JM, Eschwege E, Jacqueson A, Richard JL, Rosselin G. Body mass, blood pressure, glucose, and lipids. Does plasma insulin explain their relationships? *Arteriosclerosis* 1987; **7**: 197–202.
31 Chen CH, Tsai ST, Chou P. Correlation of fasting serum C-peptide and insulin with markers of metabolic syndrome-X in a homogenous Chinese population with normal glucose tolerance. *Int J Cardiol* 1999; **68**: 179–186.
32 Wallace TM, Levy JC, Matthews DR. Use and abuse of HOMA modeling. *Diab Care* 2004; **27**: 1487–1495.
33 Grillo CA, Piroli GG, Hendry RM, Reagan LP. Insulin-stimulated translocation of GLUT4 to the plasma membrane in rat hippocampus is PI3-kinase dependent. *Brain Res* 2009; **1296**: 35–45.
34 Lucignani G, Namba H, Nehlig A, Porrino LJ, Kennedy C, Sokoloff L. Effects of insulin on local cerebral glucose utilization in the rat. *J Cereb Blood Flow Metab* 1987; **7**: 309–314.
35 Baker LD, Cross DJ, Minoshima S, Belongia D, Watson GS, Craft S. Insulin resistance and Alzheimer-like reductions in regional cerebral glucose metabolism for cognitively normal adults with prediabetes or early type 2 diabetes. *Arch Neurol* 2011; **68**: 51–57.
36 Anticevic A, Cole MW, Murray JD, Corlett PR, Wang XJ, Krystal JH. The role of default network deactivation in cognition and disease. *Trends Cogn Sci* 2012; **16**: 584–592.
37 Fransson P, Marrelec G. The precuneus/posterior cingulate cortex plays a pivotal role in the default mode network: Evidence from a partial correlation network analysis. *NeuroImage* 2008; **42**: 1178–1184.
38 Utevsky AV, Smith DV, Huettel SA. Precuneus is a functional core of the default-mode network. *J Neurosci* 2014; **34**: 932–940.
39 Cavanna AE, Trimble MRThe precuneus: a review of its functional anatomy and behavioural correlates*Brain* 2006; 129: 564–583.
40 Sperling RA, Laviolette PS, O'Keefe K, O'Brien J, Rentz DM, Pihlajamaki M *et al.* Amyloid deposition is associated with impaired default network function in older persons without dementia. *Neuron* 2009; **63**: 178–188.
41 Wang L, Brier MR, Snyder AZ, Thomas JB, Fagan AM, Xiong C *et al.* Cerebrospinal fluid Abeta42, phosphorylated Tau181, and resting-state functional connectivity. *JAMA Neurol* 2013; **70**: 1242–1248.
42 Musen G, Jacobson AM, Bolo NR, Simonson DC, Shenton ME, McCartney RL *et al.* Resting-state brain functional connectivity is altered in type 2 diabetes. *Diabetes* 2012; **61**: 2375–2379.